

An Opportunity to Enhance Rural Electrification in sub-Saharan Africa through the Local Manufacture of a Flywheel Energy Storage System

Richard Okou¹, Adoniya Benaya Sebitosi², Pragasen Pillay³

¹Senior Research Officer, Department of Electrical Engineering, University of Cape Town, Rondebosch 7701, South Africa

Corresponding author email: Richard.okou@uct.ac.za

²Senior Lecturer, Centre for Renewable and Sustainable Energy Studies, Department of Mechanical and Mechatronics Engineering, University of Stellenbosch, Matieland, 7602, South Africa

³Professor and Senior Hydro Quebec Chair, Department of Electrical and Computer Engineering, Concordia University, Montreal, Quebec Canada H4G 2M1

ABSTRACT

This paper presents the design and prototyping of a flywheel energy storage system using locally available materials and commodity goods commonly available in sub-Saharan Africa. The essence of the study is to enhance the energy storage component of Solar Home Systems (SHS) to ensure long life, environmentally friendly and deeper cycles for the system. This is vital as most of the rural communities in sub-Saharan Africa use SHS for lighting with the battery being the weakest link requiring frequent maintenance or replacement. The system consists of a flywheel rotor, electrical machine, energy efficient bearings, power electronics and containment structure for safety. An Axial Flux Permanent Magnet Machine (AFPM) with Brushless DC (BLDC) was chosen and the driving factors of choice were, ease of construction and maintenance, high power and torque densities. The BLDC drive was designed simulated and tested showing good response times. The components were prototyped independently, assembled and tested reaching up to 25% of the energy requirement.

Keywords: Energy Conversion, Energy Storage, Flywheel, Permanent Magnet Machines, Rural Electrification

1.0 INTRODUCTION

Two billion people in the world today lack access to electricity and other modern sources of energy. In South Africa alone, 34% do not have access to electricity (Winkler, 2005) and in the case of Uganda; only 6% have access to electricity and only 1% from rural areas (Kamese, 2004), 2% for Zambia and 5% for Kenya and Mali (Martinot, 2007). These non-electrified rural areas in sub-Saharan Africa are usually far away from the grid, are mountainous, or not considered economically viable. They are gifted by nature giving rise to renewable energy resources that can be harnessed to produce electricity from anywhere. This means that unlike traditional central power generation, some renewable energy can be generated close to where it is required and massive savings on transmission infrastructure and power delivery losses can be realized. The intermittent nature of the resources however, means that power is often generated before or after it is required (Post, 1996). Therefore, in order to reliably utilize these resources, suitable energy storage must be available.

The lead acid battery, which is extensively used in sub-Saharan Africa in SHS, is characterized by high maintenance costs, low depth of discharge, limited number of charge cycles and short life spans. In addition, the disposal of used the lead acid batteries has serious environmental implications. Needless to say, energy storage is by far one of the biggest challenges to the viable exploitation of renewable energy resources. The development of low-cost, long-life storage systems that are also environmentally friendly will mitigate these shortcomings particularly for rural sub-Saharan Africa.

2.0 SYSTEM DESCRIPTION

The flywheel energy storage system consists of a flywheel rotor coupled to a three phase AFPM machine. The flywheel rotor provides the required inertia to store the designed energy and the electrical machine is charged with the energy conversion in the system. For the experimental set up, the machine is powered through a 100A rectifier dc supply via a three phase bidirectional inverter driven by Pulse Width Modulation (PWM) switching from control desk as shown in Figure.1.

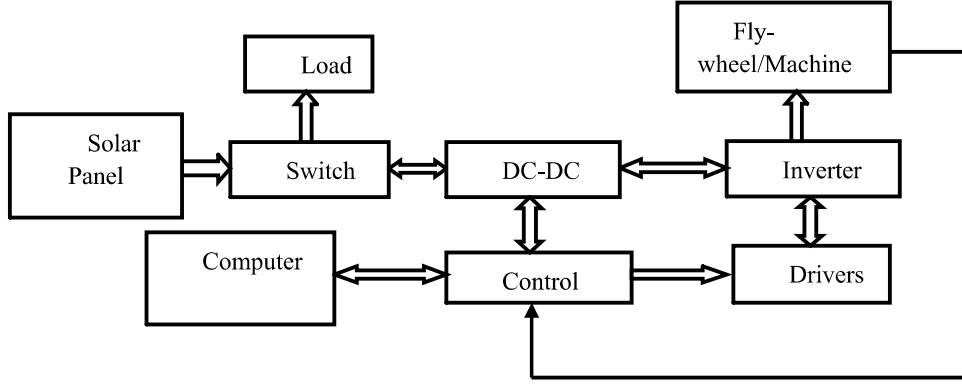


Figure 1: General schematic of flywheel system

The control of the system is determined by the rotor position of the magnets given by the hall sensor magnets and the PWM switching of the inverter switches. The amount of energy in the system increases exponentially with speed hence the need to have a high operating speed limit. This is illustrated in Equation 1. In principle, the amount of energy stored in a flywheel is given by (Genta, 1985).

$$E = \frac{1}{2} J \omega^2 \quad (1)$$

Where J is the moment of inertia and ω is the rotational speed of the flywheel rotor

The system's operating speed range is between 8,000 rpm to 25,000 rpm storing up to 300Wh. During motor mode, the flywheel system is ramped to its maximum designed speed when the PV panel (dc source) transfers energy to the machine. During generator mode, the supply is switched off, a load is connected as shown in Figure 1. This in turn absorbs energy from the flywheel hence reducing its speed. For the case when no load is connected, the speed drops due to the rotational losses. As the voltage magnitude and frequency of the machine are directly proportional to the speed of rotation, a DC-DC converter is required to ensure constant voltage at the load side. However, in the final system, the DC-DC converter was neglected and the load was supplied directly. The ability of a flywheel to reach high speeds is mainly dependent on the maximum strength of the material, which is given by Equation 2 below (Genta, 1985).

$$\sigma = \rho r^2 \omega^2 \quad (2)$$

Where σ is the ultimate tensile strength of the rotor material, ρ is the density of the flywheel rotor material, r is the radius of the flywheel rotor and ω is the rotational speed of the flywheel. In addition, the energy density of a rotor at burst speed is dependent only on the flywheel design and the characteristics of the material (Genta, 1985) as shown in Equation 3 below.

$$\left(\frac{e}{m} \right) = K \frac{\sigma}{\rho} \quad (3)$$

Where $\left(\frac{e}{m} \right)$ the energy density and K is the shape factor

From Equation 3 it can be seen that the energy stored is proportional to the strength of the material. In fact, structural integrity is by far the biggest challenge to this technology.

3.0 PROTOTYPING OF FLYWHEEL SYSTEM

3.1 Flywheel Rotor Construction

There are various methods that have been used in manufacturing composites for flywheel rotors (Genta 1982, Johnson 2008, Thoole 1993). The failure of these structures is dependent on a number of parameters. Composite structures with radially thin rims made by winding high strength fibres in the circumferential direction achieve higher specific energy than other composite structures (Yai *et al*, 2008). These rims are easily manufactured with low cost however thicker rims cannot be achieved due to limited radial strength (Arvin *et al*, 2006). Multi-ring rotors exhibit natural frequencies far beyond the operating speed range (Danfelt *et al*, 1977) and the residual thermal stresses are often a sizeable percentage of the radial tensile strength of the composite and must be accounted for (Arvin *et al* 2006, Ha *et al* 2007). The radial strength can also be improved by using layered laminates, woven fabrics among others; however this complex fibre laying can lead to delamination and micro cracking at relatively low stress levels (Kitade 2000, Genta 1981).

In this study, a laminating method is considered to improve the radial strength created when using the filament wound. This method makes use of a vacuum and autoclave assisted resin transfer moulding process. The flywheel was manufactured using layers of woven fibre glass and epoxy resin to a fibre to resin ratio of at least 70-74%. The woven fibre is layered in several directions to improve the strength in all directions with acceptable thickness levels. The final geometry is then CNC machined to specification. In the first instance, the fibre was layered and resin injected. Due to the viscosity of the resin and compactness of the fibre, the resin was not able to penetrate the entire flywheel. This created voids in the product. To eliminate the reoccurrence of the voids, the profile was subdivided into six parts. The six parts were manufactured separately and joined using high strength adhesive. This was sufficient to withstand the axial forces exerted on the flywheel. The profile was then CNC machined to create the profile shown in Figure 2.



Figure 2: Complete hyperbolic profile using layered technique

With this technique, a high fibre to resin ratio was achieved. The final product had an inner diameter of 35mm, outer diameter of 460mm with a mass of 17.6kg. The increased inner diameter meant a change in the shaft connection used. An elastomeric bushing was utilised to reduce on the radial elongation between the flywheel and shaft. These bushings for shaft-flywheel connections have been explored in (Thoole 1993, Fu *et al* 2009) with no inherent problems.

3.2 Electrical Machine Construction

The electrical machine is made up to of two rotor disks. Each rotor disk is 150mm OD, 80mm ID and is made from high strength carbon steel. The permanent magnets placed on the disks have an arc segment of 75° and are 10mm thick. The magnets are grade 40 (maximum energy product 40MGoe), NiCuNi plating with operating temperature of 120°C. These were glued onto rotor disks and epoxy resin used between the PMs to improve on the retention of the magnets. The attractive forces from the magnets are contained by use of shoulders in the shaft design. The flux path is from one pole through the windings to the second disk and back through the back iron.

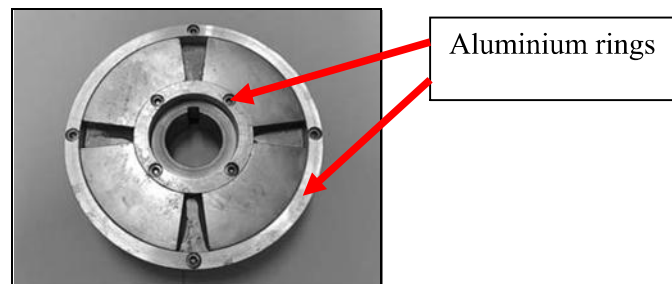


Figure 3: Complete rotor disk structure

The aluminium rings are used to further increase the retention of the magnets. A coreless stator was considered to eliminate core losses. Concentrated windings were used to produce a flat back EMF waveform. The stator was constructed from a 1.6mm conductor size with class H insulation. It has 6 coils per phase with 16 turns per coil.

3.3 Assembly of Flywheel System

For safety concerns the flywheel system was tested in a vacuum containment system as shown in Figure 4. All the assembled components are stand alone units. The power and signal cables are taken through circular connectors. The power cables are isolated from the signals to avoid interference.

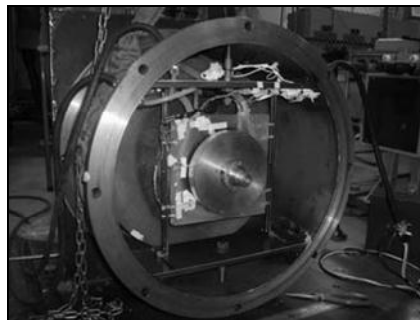


Figure 4: Assembly of the flywheel system.

4.0 SIMULATION AND EXPERIMENTAL RESULTS

4.1 Flywheel Drive System Simulation

The following set of results shows tests conducted on the overall flywheel system, i.e. DC-DC converter and BLDC drive. Figure 5 shows the speed, voltage and current for start up and motor mode of operation. When operating the motor below 8,000 rpm, the motor is current limited to a maximum of 10A. When surpassing 8,000 rpm, the machine enters the constant power region whereby the machines power is limited to rated power, 100W. Figure 6 shows the steps in output voltage of the DC-DC converter as the voltage is firstly stepped from 0V to 10V, then at 0.8seconds it is stepped from 10V to 33V, to achieve the desired speed response.

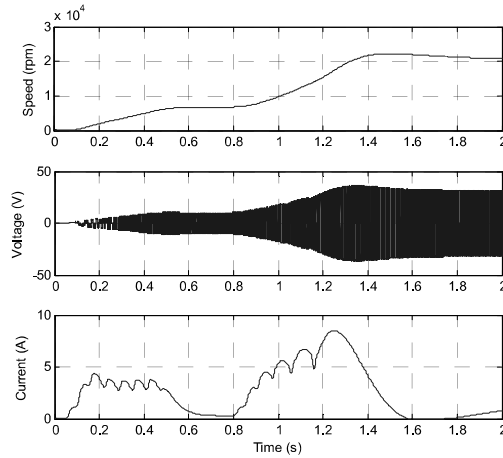


Figure 5: Start-up and motor mode of operation

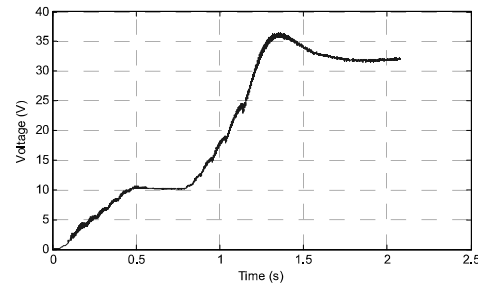


Figure 6: Output Voltage for start-up and motor mode of operation

Figure 7-9 shows the system in the generator mode of operation. In this test, the speed is initially at 22,000 rpm, after which power is required at the load end. As power is drawn from the flywheel, the machine speed steadily decreases until it reaches 8,000 rpm, as shown in Figure 7. At 8,000 rpm, the system is disconnected from the load. Figure 8 shows the voltage at the BLDC drive-end of the DC-DC converter. As power is drawn, the machines speed decreases and so does the back-emf. As this decreases, the control attempts to maintain an output voltage at the consumer-end of 12V, as shown in Figure 9.

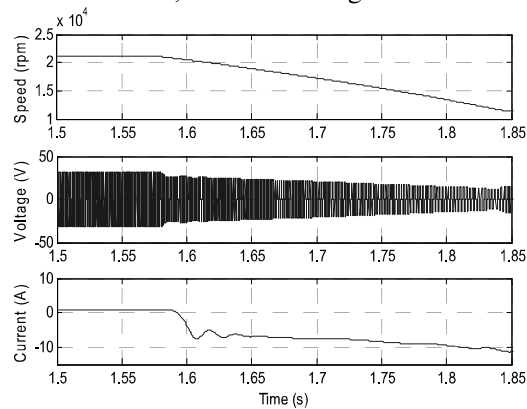


Figure 7: Generator mode of operation

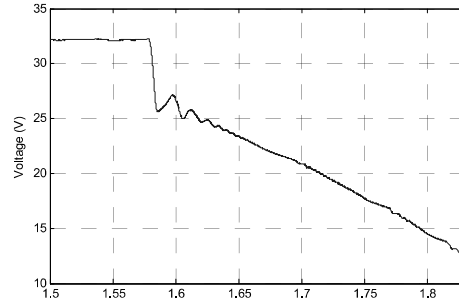


Figure 8: DC voltage at terminals of BLDC drive for generator mode of operation

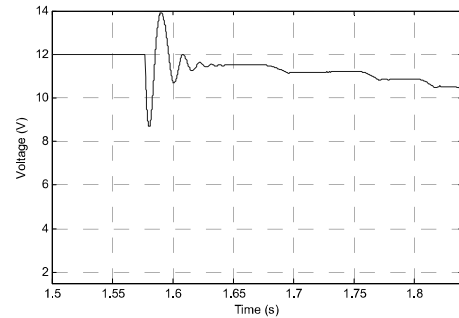


Figure 9: Consumer voltage for generator mode of operation

4.2 Experimental Rundown Curve

The system was accelerated to maximum speed of 6,000 rpm at reduced air pressure. Figure 10 shows the rundown curve of the flywheel system which was able to store up to 77Wh which represents 25% of the designed energy requirement. The system was not accelerated to higher speeds due to the vibrations from the assembled system. Figure 11 shows the mechanical losses which cause the system to run down at no load.

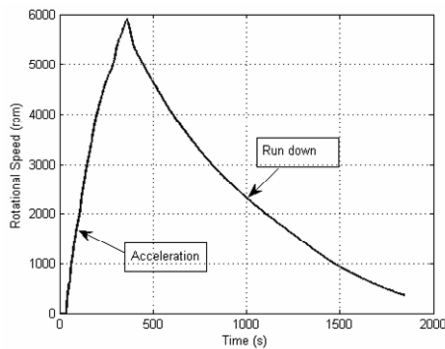


Figure 10: The run down curve.

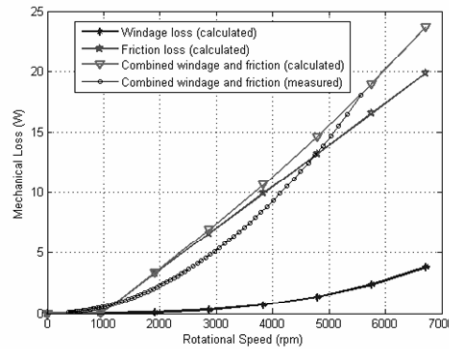


Figure 11: System losses

The measured mechanical loss shows an exponential profile, which signifies the existence of windage loss at increased speeds. This is attributed to the pressure leakages existing in the test rig. The vacuum pump used was not able to hold the vacuum consistently. In addition, the contact energy efficient bearings used further increased the losses.

5.0 CONCLUSION

A flywheel system was prototyped storing up to 25% of the energy requirement. The system was unable to reach higher speeds due to vibrations and frictional losses. The vibrations are attributed to the uneven distribution in the fiber arrangement of the flywheel while the frictional losses are mainly from the energy efficient contact bearings and windage loss at high speed. These bearings were selected to further reduce the cost of the system and complexity in maintenance. The loss analysis performed on the system showed increased losses at high speed. Future work includes investigating low cost magnetic bearing to reduce on the idling losses and improvement of control system to utilize the availability of solar Photo Voltaic (PV) throughout the day.

6.0 REFERENCES

- Arvin, A. C., Bakis, C. E., (2006), *Optimal design of press-fitted filament wound composite flywheel rotors*, Elsevier Composite Structures, vol. 72, 47–57.
- Bai, Y., Gao, Q., Li, H., Wu, Y., Xuan, M., (2008), *Design of composite flywheel rotor*, Mech. Eng. **3**(3), 288–292.
- Danfelt, E.L., Hewes, S.A. and Chou, T.W., (1977), *Optimization of composite flywheel design*, Int. J. Mech. Sci. vol. 19, 69–78.
- Fu, S.Y., Lauke, B., and Mai, Y.W., (2009), *Science and Engineering of Short Fibre Reinforced Polymer Composites*, Woodhead.
- Genta, G., (1985), *Kinetic energy storage, Theory and practice of advanced flywheel systems*, Butterworth & Co. Ltd.
- Genta, G., (1982), *Spin tests on medium energy density flywheels*, "Composites. Butterworth & Co (Publishers) Ltd.
- Genta, G., (1981), *The shape factor of composite material filament-wound flywheels*, "Composites.
- Ha, S.K., Kim, D.J, and Sung, T.H., (2001), *Optimum design of multi-ring composite flywheel rotor using a modified generalized plane strain assumption*, Elsevier, International Journal of Mechanical Sciences, vol.43, 993–1007.
- Johnson, D., (2008), *Design considerations and implementation of an electromechanical battery system*, Ph.D. dissertation, Dept. Electrical Engineering, University of Cape Town.
- Kamese, G., (2004), *Renewable Energies in Uganda*, March.
- Kitade, S., (2000), *Comprehensive composite materials*, vol. 6. Elsevier, Chapter 6 Flywheel, pp.571–580.
- Martinot, E., (2007), *Global status report*, Renewable,
- Post, R. F., 1996, *A New Look at an Old Idea*, Electromechanical battery Science and Technology Review, 13–19.
- Thoolem, F.J.M., (1993), *Development of an advanced high speed flywheel energy storage system*, " Ph.D. dissertation, Eindhoven University of Technology, Netherlands.
- Winkler, H., 2005, *Renewable energy policy in South Africa: Policy options for renewable electricity*, Energy Policy, vol. 33, 27–38.